



THE UNIVERSITY *of* EDINBURGH

Edinburgh Research Explorer

Elastic properties of suspended multilayer WSe₂

Citation for published version:

Zhang, R, Koutsos, V & Cheung, R 2016, 'Elastic properties of suspended multilayer WSe₂', *Applied Physics Letters*, vol. 108, 042104. <https://doi.org/10.1063/1.4940982>

Digital Object Identifier (DOI):

[10.1063/1.4940982](https://doi.org/10.1063/1.4940982)

Link:

[Link to publication record in Edinburgh Research Explorer](#)

Document Version:

Publisher's PDF, also known as Version of record

Published In:

Applied Physics Letters

General rights

Copyright for the publications made accessible via the Edinburgh Research Explorer is retained by the author(s) and / or other copyright owners and it is a condition of accessing these publications that users recognise and abide by the legal requirements associated with these rights.

Take down policy

The University of Edinburgh has made every reasonable effort to ensure that Edinburgh Research Explorer content complies with UK legislation. If you believe that the public display of this file breaches copyright please contact openaccess@ed.ac.uk providing details, and we will remove access to the work immediately and investigate your claim.



Elastic properties of suspended multilayer WSe₂

Rui Zhang, Vasileios Koutsos, and Rebecca Cheung

Citation: [Applied Physics Letters](#) **108**, 042104 (2016); doi: 10.1063/1.4940982

View online: <http://dx.doi.org/10.1063/1.4940982>

View Table of Contents: <http://scitation.aip.org/content/aip/journal/apl/108/4?ver=pdfcov>

Published by the [AIP Publishing](#)

Articles you may be interested in

[Electrostatic properties of two-dimensional WSe₂ nanostructures](#)

J. Appl. Phys. **119**, 035301 (2016); 10.1063/1.4940160

[Current fluctuation of electron and hole carriers in multilayer WSe₂ field effect transistors](#)

Appl. Phys. Lett. **107**, 242102 (2015); 10.1063/1.4937618

[Vapor-transport growth of high optical quality WSe₂ monolayers a](#)

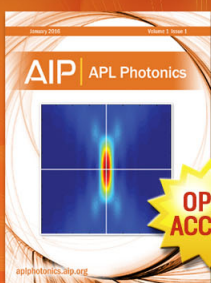
APL Mater. **2**, 101101 (2014); 10.1063/1.4896591

[WSe₂ field effect transistors with enhanced ambipolar characteristics](#)

Appl. Phys. Lett. **103**, 103501 (2013); 10.1063/1.4820408

[Modulation periodicity dependent structure, stress, and hardness in NbN/W₂N nanostructured multilayer films](#)

J. Appl. Phys. **109**, 123525 (2011); 10.1063/1.3598083



Launching in 2016!

The future of applied photonics research is here

AIP | APL
Photonics

Elastic properties of suspended multilayer WSe₂

Rui Zhang,^{1,a)} Vasileios Koutsos,² and Rebecca Cheung¹

¹Scottish Microelectronics Centre, Alexander Crum Brown Road, The University of Edinburgh, King's Buildings, Edinburgh EH9 3FF, United Kingdom

²Institute for Materials and Processes, School of Engineering, The University of Edinburgh, King's Buildings, Edinburgh EH9 3FB, United Kingdom

(Received 12 November 2015; accepted 17 January 2016; published online 27 January 2016)

We report the experimental determination of the elastic properties of suspended multilayer WSe₂, a promising two-dimensional (2D) semiconducting material combined with high optical quality. The suspended WSe₂ membranes have been fabricated by mechanical exfoliation of bulk WSe₂ and transfer of the exfoliated multilayer WSe₂ flakes onto SiO₂/Si substrates pre-patterned with hole arrays. Then, indentation experiments have been performed on these membranes with an atomic force microscope. The results show that the 2D elastic modulus of the multilayer WSe₂ membranes increases linearly while the prestress decreases linearly as the number of layers increases. The interlayer interaction in WSe₂ has been observed to be strong enough to prevent the interlayer sliding during the indentation experiments. The Young's modulus of multilayer WSe₂ (167.3 ± 6.7 GPa) is statistically independent of the thickness of the membranes, whose value is about two thirds of other most investigated 2D semiconducting transition metal dichalcogenides, namely, MoS₂ and WS₂. Moreover, the multilayer WSe₂ can endure ~ 12.4 GPa stress and $\sim 7.3\%$ strain without fracture or mechanical degradation. The 2D WSe₂ can be an attractive semiconducting material for application in flexible optoelectronic devices and nano-electromechanical systems. © 2016 Author(s). All article content, except where otherwise noted, is licensed under a Creative Commons Attribution 3.0 Unported License. [<http://dx.doi.org/10.1063/1.4940982>]

Two-dimensional (2D) materials have triggered great interest in the application of flexible electronic devices and nano-electromechanical systems (NEMS) in recent years, due to their unique physical properties (ultralow weight, high Young's modulus, and high strength) and flexibility. The most widely studied 2D material so far is graphene because of its extraordinary physical properties (Young's modulus of ~ 1 TPa and breaking strength of 100–120 GPa)^{1,2} and high mobility,³ and there has been a great quantity of research related to graphene based flexible devices^{4,5} and NEMS.^{6–8} However, pristine graphene does not have a bandgap,⁹ which limits its applications in certain fields requiring a semiconducting material. As a potential substitute material of graphene, the 2D semiconducting transition metal dichalcogenides (TMDs) with an intrinsic bandgap,^{10,11} such as MoS₂, WS₂, and WSe₂, attract increasing attention, especially in electronic and optoelectronic applications.^{12–15}

2D WSe₂ (normally exfoliated from the synthetic WSe₂ crystals grown by chemical vapor transport method), as a semiconductor with high optical quality (much higher electroluminescence efficiency than natural MoS₂,^{16,17} higher photoluminescence (PL) intensity than synthetic WS₂ and natural MoS₂,¹⁰ higher photo-conversion efficiency than natural MoS₂^{18,19}), is a promising 2D material for application in optoelectronic devices, such as photodetectors, photovoltaics, and light-emitting diodes (LEDs). Simultaneously, under tensile strain, monolayer WSe₂ remains a direct

bandgap material with a bandgap decrease rate of ~ 8 meV/% and multilayer WSe₂ undergoes an indirect to direct bandgap transition,²⁰ while monolayer MoS₂ shows a direct to indirect bandgap transition with a higher bandgap decrease rate of ~ 45 meV/% (PL intensity decreases rapidly with strain).²¹ Since the strain induced bandgap change will influence the resistivity of 2D materials,²² the smaller rate of bandgap change under strain of 2D WSe₂ makes it a great contender for flexible electronic/optoelectronic device applications. Although a lot of research has been done to study the electrical and optical properties of the 2D TMDs,^{23–28} the investigations relevant to quantifying their mechanical properties experimentally (MoS₂^{29–31} and WS₂³¹) are still quite few. So far, the experimental measurement of elastic properties of 2D WSe₂ has not been reported yet. In this work, we report the in-plane elastic properties of exfoliated multilayer WSe₂ extracted from nanoindentation experiments. Our experiment aims to pave the way for the design and fabrication of a 2D WSe₂ based flexible device and NEMS.

The indentation experiments have been performed on multilayer WSe₂ membranes suspended over circular holes with an atomic force microscope (AFM). First, 280 nm SiO₂ has been grown on Si substrates by thermal oxidation, which gives the optimal color contrast between WSe₂ flakes and the substrates.^{32,33} Then, the SiO₂ layers have been patterned with circular hole (1.55 μ m and 2.6 μ m in diameter, 220 nm in depth) arrays by photolithography and reactive ion etching (see Fig. S1 of the supplementary material).³⁴ After etching, the photoresist has been stripped by sonication in acetone, isopropyl alcohol (IPA), and de-ionized (DI) water sequentially. Then, the substrates have been soaked in Piranha

^{a)}Author to whom correspondence should be addressed. Electronic mail: rui.zhang@ed.ac.uk

solution for 30 min and rinsed in DI water to remove organic residues, followed by O_2 plasma treatment to increase the interaction between WSe_2 flakes and SiO_2 surface by removing the ambient adsorbates on SiO_2 surface.^{35,36} Thereafter, multilayer WSe_2 flakes have been exfoliated mechanically from bulk WSe_2 crystals (supplied by 2D Semiconductors, Inc.) and transferred onto the hole arrays in SiO_2/Si substrates with a polydimethylsiloxane (PDMS) stamp^{37,38} (see Fig. S2 of the supplementary material).³⁴ Contact mode AFM (Bruker: MultiMode, Nanoscope IIIa) with a set-point force of ~ 25 nN has been used to obtain the topography of WSe_2 flakes on substrates and determine the thickness of the flakes. The reason why contact mode instead of tapping mode has been chosen is to provide accurate results for the thickness measurement.³⁹ The number of layers of the corresponding flakes has been derived by dividing the measured thickness by the interlayer distance. An interlayer distance of 0.70 nm for WSe_2 ^{40,41} has been adopted for calculation.

Fig. 1(a) shows the multilayer WSe_2 flakes, which have been transferred onto the substrate pre-patterned with an array of holes, forming several suspended WSe_2 membranes over the holes. Fig. 1(b) presents the AFM image of the corresponding WSe_2 flake in the square area of Fig. 1(a), while Fig. 1(c) shows the magnified AFM topography image of a suspended area of a 6-layer WSe_2 membrane over a $1.55 \mu m$ diameter hole. No visible bubbles, wrinkles, or residue particles have been found on the membranes, which benefits from the appropriate pressure control during the all-dry transfer process.³⁷ The height profile superimposed in the AFM image of Fig. 1(c) shows a uniform height around the edge of the hole, indicating that the membrane adheres tightly to the edge of the hole possibly by van der Waals interactions (dispersion forces or dipole interactions or both) with the substrate. The Raman measurements have been performed in a confocal Raman spectrometer (inVia Renishaw)

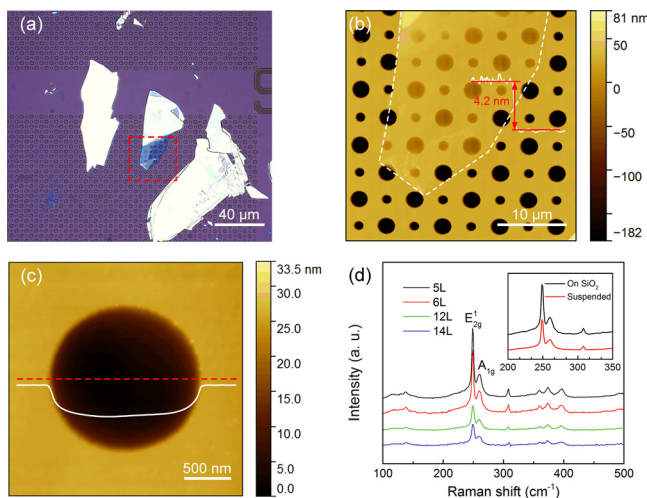


FIG. 1. (a) Optical image of WSe_2 flakes transferred onto pre-patterned SiO_2/Si substrate. (b) AFM image of the corresponding WSe_2 flake inside the square area of (a). (c) AFM image of a WSe_2 membrane suspended over a hole and a superimposed height profile (along the dashed line) shows a step height of ~ 30 nm. (d) Raman spectra of the suspended WSe_2 flakes with different number of layers in the range of $100\text{--}500\text{ cm}^{-1}$. The inset shows the Raman spectra of supported area and suspended area of a 5-layer WSe_2 flake in the range of $200\text{--}350\text{ cm}^{-1}$. Spectra are offset vertically for clarity.

with a $100\times$ magnification objective in air environment. The wavelength of the laser is 514 nm, and the laser power has been kept at ~ 0.2 mW. The Raman spectra of the transferred multilayer WSe_2 flakes suspended over the holes are shown in Fig. 1(d). The in-plane mode E_{2g}^1 (248.7 cm^{-1}), out-of-plane mode A_{1g} (259.6 cm^{-1}),⁴² and a weak peak at 308.2 cm^{-1} arising from the interlayer interaction⁴⁰ have been observed. No Raman splitting of the E_{2g}^1 mode has been observed, indicating no large strain ($>1\%$) exists in the transferred WSe_2 flakes.²⁰ The inset of Fig. 1(d) compares the Raman spectra of supported area and suspended area of a 5-layer WSe_2 flake. Peak position shift of E_{2g}^1 and A_{1g} modes has not been found, which suggests similar strain exists in the supported and suspended areas.

To obtain the elastic properties of the suspended membranes, indentation experiments have been conducted. Prior to the indentation, the samples have been scanned for 1 h under AFM in order to minimize the thermal drift of the piezoelectric scanner. Then, the tip of an AFM probe with a radius r_{tip} of 81 nm (NuNano: Scout 350 LowRes) has been located in the center of a suspended area of a membrane, and the membrane has been indented with a loading/unloading rate of 100 nm/s repeatedly for several cycles (as illustrated in Fig. 2(a)). During the measurement, no hysteresis has been found in the loading and unloading curves, which indicates that no plastic deformation has occurred to the membranes and the membranes have not slid over the margin of holes. The indentation depth at the center of a membrane has been determined by $\delta = \Delta Z - d$, where ΔZ is the displacement of the piezoelectric scanner as the AFM probe starts to contact with the membrane (see the supplementary material for the determination of contact point),³⁴ and d is the deflection of the AFM probe. The force applied from the AFM tip onto the membrane has been derived from $F = k \times d$, where k is the spring constant of the corresponding AFM probe (35.7 N/m), which has been calibrated via a reference cantilever with a known spring constant (Bruker: CLFC-NOBO). Representative force F versus displacement ΔZ curves on a suspended WSe_2 membrane and SiO_2/Si substrate are shown in Fig. 2(b). When the AFM probe indents towards the stiff substrate, the probe deflection d is assumed to be equal to the displacement of the scanner ΔZ , which has been used to calibrate the sensitivity of the photodetector of AFM.

Since WSe_2 owns three-fold rotation symmetry and the suspended area of WSe_2 has circular symmetry, each WSe_2 membrane has been modelled as a film with isotropic in-plane mechanical properties. Fig. 2(c) shows the representative force-deformation curves obtained from WSe_2 membranes with different number of layers, which can be approximated with the Schwering-type solution as^{2,43,44}

$$F = (\sigma_0^{2D} \pi) \delta + \left(E^{2D} \frac{q^3}{r^2} \right) \delta^3, \quad (1)$$

where σ_0^{2D} is the pretension, r is the radius of the hole, E^{2D} is the 2D elastic modulus, ν is the Poisson's ratio (0.19 (Refs. 45 and 46) for WSe_2), and q is a dimensionless constant determined by $q = 1/(1.05 - 0.15\nu - 0.16\nu^2)$. With a least square fitting of the experimental data using Eq. (1), the pretension σ_0^{2D} and 2D elastic modulus E^{2D} of the

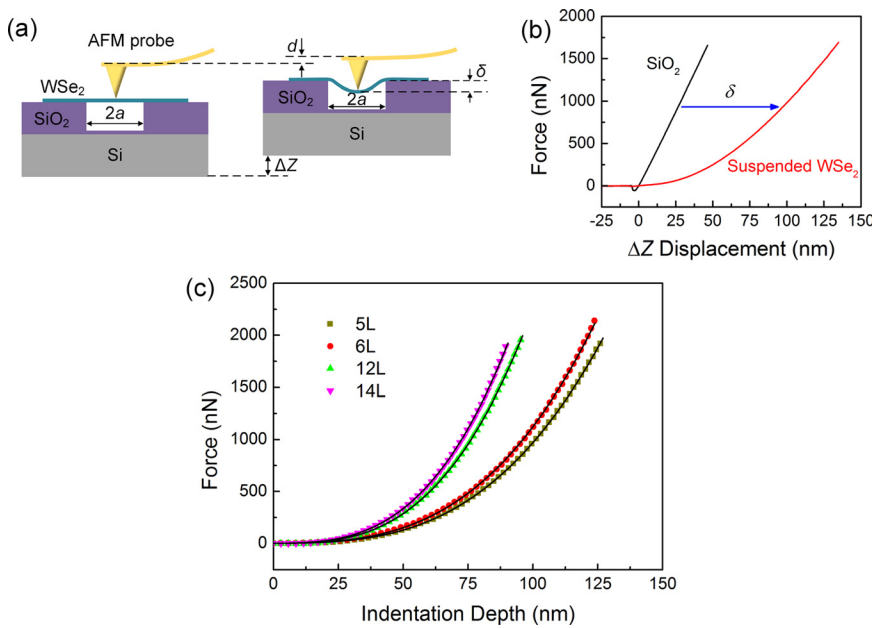


FIG. 2. (a) Schematic of the indentation experiment on a suspended WSe₂ membrane. (b) Force-displacement curves obtained on a suspended WSe₂ membrane and SiO₂/Si substrate. (c) Representative force-deformation curves for suspended WSe₂ membranes with different number of layers. The symbols correspond to the experimental data and the solid lines are fitted curves, agreeing well with the experimental results.

membranes can be derived. The fitted curves (solid lines in Fig. 2(c)) show good agreement with the experimental data, demonstrating the suitability of the chosen mechanic model. From this model, we can see the applied load has an approximate linear relationship with the indentation depth when the membrane deformation is small, while significantly follows a cubic relationship under large deformation.

To determine the variation of the mechanical properties of the suspended WSe₂ membranes, a statistical analysis has been conducted on several WSe₂ flakes with 5, 6, 12, and 14 layers. For each set of layers, the test has been done on 5 membranes with 3 different indentation depths twice, and therefore, 30 force-deformation curves have been obtained, which derives 30 values of σ_0^{2D} and E^{2D} by fitting Eq. (1) to the corresponding force-deformation curves. The results show that both the extracted 2D elastic modulus E^{2D} and pretension σ_0^{2D} are independent of the indentation depth (as shown in Fig. S5 of the supplementary material),³⁴ which verifies the WSe₂ membranes present an elastic deformation during the indentation experiments. The histograms of the derived 2D elastic modulus E^{2D} and pretension σ_0^{2D} for WSe₂ membranes with different number of layers are shown in Figs. 3(a)–3(d) and Fig. S6 (see the supplementary material),³⁴ respectively, which can be fitted with the Gaussian distribution. The mean 2D elastic modulus and their standard deviations are 596 ± 23 , 690 ± 25 , 1411 ± 61 , and 1615 ± 56 N/m for 5, 6, 12, and 14-layer thick WSe₂ membranes, respectively, as shown in Fig. 3(e). The deviations are attributed to different defect densities, stacking faults in the membranes, offset of the AFM tip from the center of a membrane, and the curve fitting errors. The 2D elastic modulus of the multilayer WSe₂ membranes has been observed to increase statistically linearly as the number of layers increases. As described previously, the membranes have been found to clamp tightly over the edges of holes (no sliding over the substrates), which indicates interlayer sliding has not happened during the indentation experiments due to the interlayer interaction originating from van der Waals interactions.⁴⁷

In order to compare the elastic properties of 2D WSe₂ with the bulk materials and other materials, the 2D elastic modulus has been converted to the normal 3D Young's modulus E_Y by dividing the 2D value by the thickness of the membranes. Fig. 4(a) shows the box chart of Young's modulus E_Y for WSe₂ membranes with different number of layers. No statistical difference of E_Y among the 4 different WSe₂ membranes has been observed in our results, which indicates the Young's modulus E_Y of the WSe₂ membranes is independent of the thickness. The corresponding values are 170.3 ± 6.7 , 166.3 ± 6.1 , 167.9 ± 7.2 , and 164.8 ± 5.7 GPa for 5, 6, 12, and 14-layer thick WSe₂ membranes, respectively, which is close to the first principle simulation result.⁴⁸ Moreover, the mean value of E_Y (167.3 ± 6.7 GPa) for the multilayer WSe₂ membranes is smaller than that of multilayer MoS₂ (~ 330 GPa),²⁹ monolayer MoS₂ (~ 270 GPa),^{30,31} monolayer WS₂ (~ 270 GPa),³¹ roughly equal to one sixth of graphene (~ 1.0 TPa)^{1,2} and carbon nanotube (~ 1.0 TPa),⁴⁹ and larger than that of MoS₂ nanotube (~ 120 GPa).⁵⁰ The possible reason for smaller Young's modulus of WSe₂ compared with 2D MoS₂ and WS₂ is that the charge transfer decrease and lattice constant increase in WSe₂ induces the weakening binding between the metal and chalcogen.⁴⁶ For a given geometry of NEMS, the resonant frequency will be lower if the Young's modulus of beam is lower or density is higher.^{51,52} Thus, 2D WSe₂ with a relatively higher density value (9.32 g/cm³)⁵³ and lower Young's modulus compared with other 2D materials can be put into application of NEMS with lower resonance frequency, such as acoustic sensor⁵⁴ and loudspeakers.⁵⁵ In addition, when flexible electronics composed of 2D materials are bent or stretched, extra stress will be formed at the interface between the 2D material and soft polymeric substrates, due to the mismatch of their mechanical properties, which may weaken the reliability of the devices. 2D WSe₂ with lower Young's modulus will reduce this kind of stress under a certain amount of strain of devices and may therefore be more suitable for flexible electronics applications.

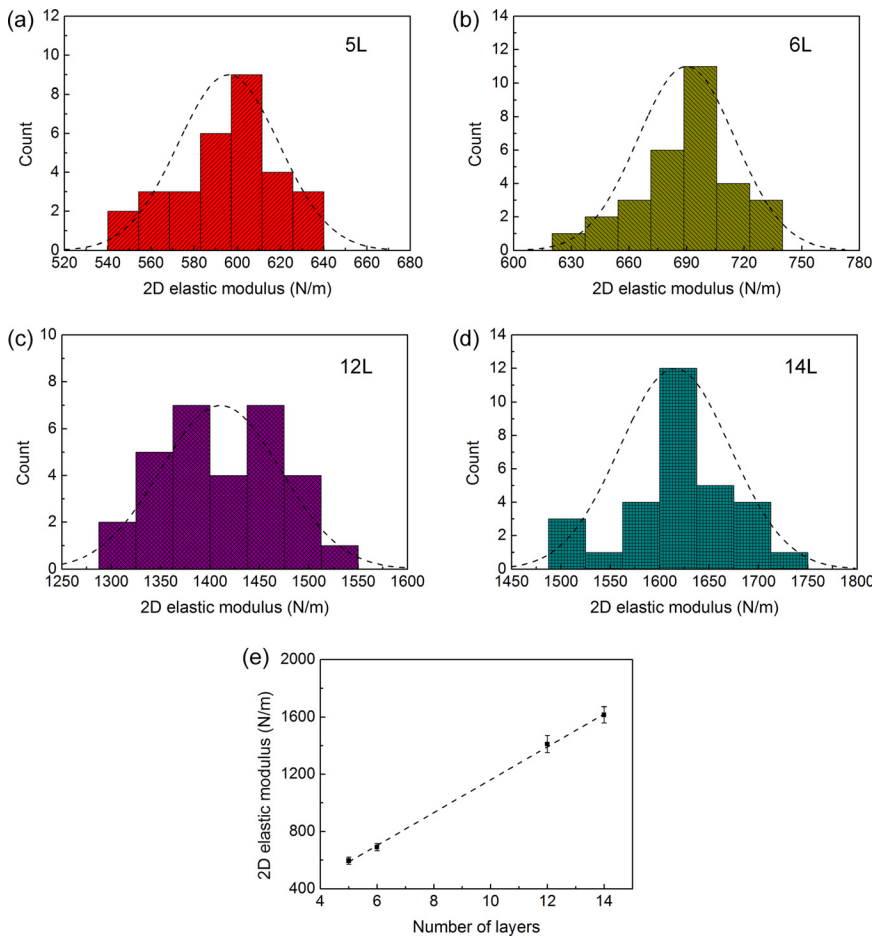


FIG. 3. Histograms of 2D elastic modulus E^{2D} acquired from the curve fitting with Eq. (1) for (a) 5-layer, (b) 6-layer, (c) 12-layer, and (d) 14-layer thick WSe₂ membranes. The dashed lines indicate the fitted Gaussian distributions. (e) 2D elastic modulus E^{2D} of WSe₂ membranes as a function of the number of layers. The error bars represent the standard deviations.

During the whole indentation experiments, the maximum force applied on these WSe₂ membranes is ~ 3200 nN. None of the membranes have been fractured and all still kept their original elastic properties under this force. The maximum stress for a circular and linear elastic membrane during an indentation experiment with a spherical indenter in the case of $r_{\text{tip}}/r \ll 1$ can be derived with the expression as⁵⁶

$$\sigma_{\text{max}}^{2D} = \sqrt{\frac{F_{\text{max}} E^{2D}}{4\pi r_{\text{tip}}}}. \quad (2)$$

Thus, the maximum stress for a 5-layer WSe₂ membrane is calculated to be ~ 43 N/m, corresponding to ~ 12.4 GPa. Assuming the stress of multilayer WSe₂ has a linear relationship with its strain ($\sigma = E_Y \epsilon$) results in the maximum strain of approximate 7.3%. Thus, the multilayer WSe₂ can at least

withstand ~ 12.4 GPa stress and $\sim 7.3\%$ strain without breaking. (The breaking stress/strain is larger than ~ 12.4 GPa/ $\sim 7.3\%$.) This means the breaking strain of 2D WSe₂ is at least three times larger than that of silicon (0.4%–2.2%)⁵⁷ and comparable with the common materials used for substrates of flexible electronics, namely, polyimide (PI) or PDMS ($\sim 7\%$),⁵⁸ implying that 2D WSe₂ is compatible with most of flexible electronic devices.

Fig. 4(b) shows the relationship between the extracted pretension and prestress (pretension divided by the thickness of the membranes) and the number of layers of WSe₂ membranes. As can be seen, in our experiments, the pretension σ_0^{2D} varies with the thickness of WSe₂ membranes and is in the same scale as the reports of Refs. 29 and 31, which employ a similar 2D materials transfer method. In addition, the prestress that originates from the mechanical exfoliation and transfer process decreases approximately linearly as the number of layers increases. During the transfer process, the pressing of PDMS stamp together with WSe₂ would have resulted in the PDMS stamp expanding laterally (see Fig. S2(c) of the supplementary material),³⁴ due to the softness of the PDMS,⁵⁹ which could have stretched the WSe₂ flakes to a certain extent. When the PDMS stamp has been peeled off from the substrate, it is likely that the stretched WSe₂ flakes adhering to the substrate by van der Waals force result in the positive pretension formed in the transferred flakes.

In conclusion, we have fabricated multilayer WSe₂ membranes suspended over circular holes. The elastic properties of WSe₂ membranes with different number of layers

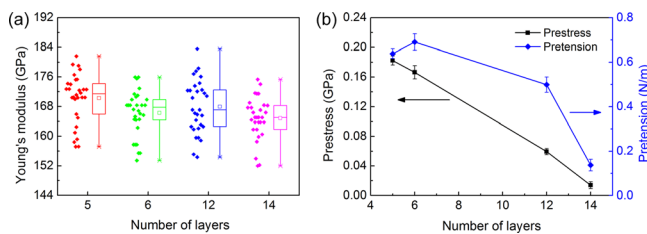


FIG. 4. (a) The box chart of Young's modulus E_Y for WSe₂ membranes with different number of layers. Each plot includes the minimum, lower quartile, median (horizontal line), mean (hollow square), upper quartile, maximum, and discrete data at the left. (b) Pretension and prestress for the corresponding multilayer WSe₂ membranes.

have been determined employing nanoindentation experiments. The results show that although the prestress decreases approximately linearly as the number of layers increases, the Young's modulus is independent of the number of layers, which indicates the interlayer interaction is strong enough to prevent the interlayer sliding. The Young's modulus of multilayer WSe₂ is about two thirds of other most investigated 2D semiconducting TMDs, namely, MoS₂ and WS₂, and one sixth of graphene and carbon nanotube. During the experiments, the WSe₂ membranes have withstood ~ 12.4 GPa stress and $\sim 7.3\%$ strain without breaking or mechanical degradation. 2D WSe₂ can be an attractive alternative for graphene in some applications requiring flexible semiconducting materials, such as bendable transistors, photodetectors, photovoltaics, and NEMS.

We would like to thank the financial support of UK Engineering and Physical Sciences Research Council (EPSRC) for this work. We acknowledge Atif Syed's assistance with the AFM tip characterization.

- ¹G.-H. Lee, R. C. Cooper, S. J. An, S. Lee, A. van der Zande, N. Petrone, A. G. Hammerberg, C. Lee, B. Crawford, W. Oliver, J. W. Kysar, and J. Hone, *Science* **340**, 1073 (2013).
- ²C. Lee, X. Wei, J. W. Kysar, and J. Hone, *Science* **321**, 385 (2008).
- ³K. S. Novoselov, A. K. Geim, S. Morozov, D. Jiang, Y. Zhang, S. a. Dubonos, I. Grigorieva, and A. Firsov, *Science* **306**, 666 (2004).
- ⁴S. Bae, H. Kim, Y. Lee, X. Xu, J.-S. Park, Y. Zheng, J. Balakrishnan, T. Lei, H. R. Kim, Y. I. Song, Y.-J. Kim, K. S. Kim, B. Ozyilmaz, J.-H. Ahn, B. H. Hong, and S. Iijima, *Nat. Nanotechnol.* **5**, 574 (2010).
- ⁵K. S. Kim, Y. Zhao, H. Jang, S. Y. Lee, J. M. Kim, K. S. Kim, J.-H. Ahn, P. Kim, J.-Y. Choi, and B. H. Hong, *Nature* **457**, 706 (2009).
- ⁶A. M. van der Zande, R. A. Barton, J. S. Alden, C. S. Ruiz-Vargas, W. S. Whitney, P. H. Q. Pham, J. Park, J. M. Parpia, H. G. Craighead, and P. L. McEuen, *Nano Lett.* **10**, 4869 (2010).
- ⁷C. Y. Chen, S. Rosenblatt, K. I. Bolotin, W. Kalb, P. Kim, I. Kymissis, H. L. Stormer, T. F. Heinz, and J. Hone, *Nat. Nanotechnol.* **4**, 861 (2009).
- ⁸J. S. Bunch, A. M. van der Zande, S. S. Verbridge, I. W. Frank, D. M. Tanenbaum, J. M. Parpia, H. G. Craighead, and P. L. McEuen, *Science* **315**, 490 (2007).
- ⁹Y. Zhang, Y.-W. Tan, H. L. Stormer, and P. Kim, *Nature* **438**, 201 (2005).
- ¹⁰W. Zhao, Z. Ghorannevis, L. Chu, M. Toh, C. Kloc, P.-H. Tan, and G. Eda, *ACS Nano* **7**, 791 (2013).
- ¹¹Q. H. Wang, K. Kalantar-Zadeh, A. Kis, J. N. Coleman, and M. S. Strano, *Nat. Nanotechnol.* **7**, 699 (2012).
- ¹²J. Yoon, W. Park, G.-Y. Bae, Y. Kim, H. S. Jang, Y. Hyun, S. K. Lim, Y. H. Kahng, W.-K. Hong, B. H. Lee, and H. C. Ko, *Small* **9**, 3295 (2013).
- ¹³H. Wang, L. L. Yu, Y. H. Lee, Y. M. Shi, A. Hsu, M. L. Chin, L. J. Li, M. Dubey, J. Kong, and T. Palacios, *Nano Lett.* **12**, 4674 (2012).
- ¹⁴S. Bertolazzi, D. Krasnozhan, and A. Kis, *ACS Nano* **7**, 3246 (2013).
- ¹⁵O. Lopez-Sanchez, D. Lembke, M. Kayci, A. Radenovic, and A. Kis, *Nat. Nanotechnol.* **8**, 497 (2013).
- ¹⁶J. S. Ross, P. Klement, A. M. Jones, N. J. Ghimire, J. Yan, D. G. Mandrus, T. Taniguchi, K. Watanabe, K. Kitamura, W. Yao, D. H. Cobden, and X. Xu, *Nat. Nanotechnol.* **9**, 268 (2014).
- ¹⁷A. Pospischil, M. M. Furchi, and T. Mueller, *Nat. Nanotechnol.* **9**, 257 (2014).
- ¹⁸S. Wi, M. Chen, D. Li, H. Nam, E. Meyhofer, and X. Liang, *Appl. Phys. Lett.* **107**, 062102 (2015).
- ¹⁹S. Wi, H. Kim, M. K. Chen, H. Nam, L. J. Guo, E. Meyhofer, and X. G. Liang, *ACS Nano* **8**, 5270 (2014).
- ²⁰S. B. Desai, G. Seol, J. S. Kang, H. Fang, C. Battaglia, R. Kapadia, J. W. Ager, J. Guo, and A. Javey, *Nano Lett.* **14**, 4592 (2014).
- ²¹H. J. Conley, B. Wang, J. I. Ziegler, R. F. Haglund, S. T. Pantelides, and K. I. Bolotin, *Nano Lett.* **13**, 3626 (2013).
- ²²A. D. Smith, F. Niklaus, A. Paussa, S. Vaziri, A. C. Fischer, M. Sterner, F. Forsberg, A. Delin, D. Esseni, P. Palestri, M. Östling, and M. C. Lemme, *Nano Lett.* **13**, 3237 (2013).
- ²³D. Ovchinnikov, A. Allain, Y. S. Huang, D. Dumcenco, and A. Kis, *ACS Nano* **8**, 8174 (2014).
- ²⁴N. Perea-López, A. L. Elías, A. Berkdemir, A. Castro-Beltrán, H. R. Gutiérrez, S. Feng, R. Lv, T. Hayashi, F. López-Urías, S. Ghosh, B. Muchharla, S. Talapatra, H. Terrones, and M. Terrones, *Adv. Funct. Mater.* **23**, 5511 (2013).
- ²⁵S. Das and J. Appenzeller, *Appl. Phys. Lett.* **103**, 103501 (2013).
- ²⁶T. Yan, X. Qiao, X. Liu, P. Tan, and X. Zhang, *Appl. Phys. Lett.* **105**, 101901 (2014).
- ²⁷H. Fang, S. Chuang, T. C. Chang, K. Takei, T. Takahashi, and A. Javey, *Nano Lett.* **12**, 3788 (2012).
- ²⁸B. Radisavljevic, A. Radenovic, J. Brivio, V. Giacometti, and A. Kis, *Nat. Nanotechnol.* **6**, 147 (2011).
- ²⁹A. Castellanos-Gomez, M. Poot, G. A. Steele, H. S. J. van der Zant, N. Agrait, and G. Rubio-Bollinger, *Adv. Mater.* **24**, 772 (2012).
- ³⁰S. Bertolazzi, J. Brivio, and A. Kis, *ACS Nano* **5**, 9703 (2011).
- ³¹K. Liu, Q. M. Yan, M. Chen, W. Fan, Y. H. Sun, J. Suh, D. Y. Fu, S. Lee, J. Zhou, S. Tongay, J. Ji, J. B. Neaton, and J. Q. Wu, *Nano Lett.* **14**, 5097 (2014).
- ³²M. M. Benameur, B. Radisavljevic, J. S. Heron, S. Sahoo, H. Berger, and A. Kis, *Nanotechnology* **22**, 125706 (2011).
- ³³P. Blake, E. W. Hill, A. H. Castro Neto, K. S. Novoselov, D. Jiang, R. Yang, T. J. Booth, and A. K. Geim, *Appl. Phys. Lett.* **91**, 063124 (2007).
- ³⁴See supplementary material at <http://dx.doi.org/10.1063/1.4940982> for the details of patterning of SiO₂/Si substrate, exfoliation, and transfer process of multilayer WSe₂, characterization of AFM tip, calibration of force-deformation curves, 2D elastic modulus and pretension at different indentation depths, and pretension distribution for WSe₂ membranes.
- ³⁵Y. Huang, E. Sutter, N. N. Shi, J. Zheng, T. Yang, D. Englund, H.-J. Gao, and P. Sutter, *ACS Nano* **9**, 10612 (2015).
- ³⁶K. Nagashio, T. Yamashita, T. Nishimura, K. Kita, and A. Toriumi, *J. Appl. Phys.* **110**, 024513 (2011).
- ³⁷A. Castellanos-Gomez, M. Buscema, R. Molenaar, V. Singh, L. Janssen, H. S. J. van der Zant, and G. A. Steele, *2D Mater.* **1**, 011002 (2014).
- ³⁸M. A. Meitl, Z. T. Zhu, V. Kumar, K. J. Lee, X. Feng, Y. Y. Huang, I. Adesida, R. G. Nuzzo, and J. A. Rogers, *Nat. Mater.* **5**, 33 (2006).
- ³⁹P. Nemes-Incze, Z. Osváth, K. Kamarás, and L. P. Biró, *Carbon* **46**, 1435 (2008).
- ⁴⁰H. Li, G. Lu, Y. Wang, Z. Yin, C. Cong, Q. He, L. Wang, F. Ding, T. Yu, and H. Zhang, *Small* **9**, 1974 (2013).
- ⁴¹W. Liu, J. Kang, D. Sarkar, Y. Khatami, D. Jena, and K. Banerjee, *Nano Lett.* **13**, 1983 (2013).
- ⁴²D. G. Mead and J. C. Irwin, *Can. J. Phys.* **55**, 379 (1977).
- ⁴³U. Komaragiri, M. R. Begley, and J. G. Simmonds, *J. Appl. Mech.* **72**, 203 (2005).
- ⁴⁴M. R. Begley and T. J. Mackin, *J. Mech. Phys. Solids* **52**, 2005 (2004).
- ⁴⁵J. Kang, S. Tongay, J. Zhou, J. Li, and J. Wu, *Appl. Phys. Lett.* **102**, 012111 (2013).
- ⁴⁶F. Zeng, W.-B. Zhang, and B.-Y. Tang, *Chin. Phys. B* **24**, 097103 (2015).
- ⁴⁷M. Kertesz and R. Hoffmann, *J. Am. Chem. Soc.* **106**, 3453 (1984).
- ⁴⁸L.-P. Feng, N. Li, M.-H. Yang, and Z.-T. Liu, *Mater. Res. Bull.* **50**, 503 (2014).
- ⁴⁹M. F. Yu, B. S. Files, S. Arepalli, and R. S. Ruoff, *Phys. Rev. Lett.* **84**, 5552 (2000).
- ⁵⁰A. Kis, D. Mihailovic, M. Remskar, A. Mrzel, A. Jesih, I. Piwonski, A. J. Kulik, W. Benoit, and L. Forró, *Adv. Mater.* **15**, 733 (2003).
- ⁵¹L. Sekaric, J. M. Parpia, H. G. Craighead, T. Feygelson, B. H. Houston, and J. E. Butler, *Appl. Phys. Lett.* **81**, 4455 (2002).
- ⁵²Y. T. Yang, K. L. Ekinci, X. M. H. Huang, L. M. Schiavone, M. L. Roukes, C. A. Zorman, and M. Mehregany, *Appl. Phys. Lett.* **78**, 162 (2001).
- ⁵³M. K. Agarwal and P. A. Wani, *Mater. Res. Bull.* **14**, 825 (1979).
- ⁵⁴E. Grady, E. Mastropaolo, T. Chen, A. Bunting, and R. Cheung, *Microelectron. Eng.* **119**, 105 (2014).
- ⁵⁵J. W. Suk, K. Kirk, Y. Hao, N. A. Hall, and R. S. Ruoff, *Adv. Mater.* **24**, 6342 (2012).
- ⁵⁶N. M. Bhatia and W. Nachbar, *Int. J. Nonlinear Mech.* **3**, 307 (1968).
- ⁵⁷T. Ando, K. Sato, M. Shikida, T. Yoshioka, Y. Yoshikawa, and T. Kawabata, paper presented at Proceedings of the 1997 International Symposium on Micromechatronics and Human Science (1997).
- ⁵⁸D.-H. Kim, J.-H. Ahn, W. M. Choi, H.-S. Kim, T.-H. Kim, J. Song, Y. Y. Huang, Z. Liu, C. Lu, and J. A. Rogers, *Science* **320**, 507 (2008).
- ⁵⁹I. D. Johnston, D. K. McCluskey, C. K. L. Tan, and M. C. Tracey, *J. Micromech. Microeng.* **24**, 035017 (2014).